

基于MIM谐振结构的高吸收率太阳能吸波器

肖功利¹, 陈康¹, 杨宏艳^{2*}, 张家荣¹, 李苗¹, 刘兴鹏¹, 陈赞辉¹¹桂林电子科技大学信息与通信学院广西高校微电子器件与集成电路重点实验室, 广西 桂林 541004;²桂林电子科技大学光电工程学院, 广西 桂林 541004

摘要 实现太阳全光谱辐射的完美吸收并尽可能少地使用光敏材料是太阳能吸波器研究的终极目标。提出了一种基于金属-电介质-金属(MIM)谐振器结构的高吸收率太阳能吸波器。该吸波器以金属钨(W)为衬底,衬底上的多层空心圆盘分别构成了金属(Ti)-相变材料(GST)-金属(Ti)或金属(Ti)-砷化镓(GaAs)-金属(Ti)的MIM谐振器结构。研究表明,GaAs和非晶态GST材料在太阳能吸波器设计方面都有极高的应用价值。该结构在0.3~2.5 μm的波长范围内的平均吸收率为97.48%,太阳能光谱加权吸收效率为98.02%;该结构在0.3~4 μm的整个工作波段内的平均吸收率为96.95%,太阳能光谱加权吸收效率为97.54%。吸收率大于95%的带宽为2.37 μm,吸收率大于90%的带宽为3.57 μm。结构自身的对称性使其具备优良的偏振无关特性,有助于吸收太阳光。此外,在0.3~2.5 μm波长范围内,该结构对入射角变化表现出稳定的响应。本研究设计的太阳能吸波器具有超宽带和高吸收率的特点,其结构简单,大大降低了制造复杂度和成本。该技术在太阳能收集与转换、光伏器件以及热发射器件等领域具有潜在的应用前景。

关键词 表面光学; 太阳能吸波器; MIM谐振结构; 高吸收率; 超宽带; 偏振无关

中图分类号 TN256 **文献标志码** A

DOI: 10.3788/AOS231934

1 引言

新能源的开发与利用一直以来是人类研究的重要领域之一。太阳能作为一种绿色、可再生能源,为缓解能源危机提供了有效途径。迄今为止,人们提出了许多将太阳辐射转化为其他能源和应用形式的方法,例如光伏和太阳能电池^[1]、光^[2-3]和热^[4-5]发电机、热发电^[6]和太阳能蒸汽发电^[7-9]、海水淡化^[10-11],以及光化学和光催化反应^[12-13]等。值得注意的是,高效的太阳能捕获^[14-16]是实现这些应用的关键。因此,研究太阳能吸波器的最终目标是在整个光谱范围内完全吸收太阳辐射,并使用尽可能少的光敏材料。在过去几年中,研究者们已经研究出了一些高效吸收太阳能辐射的方法。例如,黑色涂料被广泛使用,但它只在紫外光和可见光波段表现出高吸收率^[17-18],从而导致约28%的太阳能浪费。然而,随着科技的发展,超材料为操纵电磁波开辟了许多新途径。超材料具有许多独特的光学特性,并且已被证明可以控制电磁波的偏振态^[19-20]、幅度^[21-22]和相位^[23]。改变光振幅是控制光吸收的一种方法。因此,研究在宽光谱区域^[24-26]内实现完美吸收的超材料具有重要意义。

Landy等^[27]于2008年展示了第一个超材料完美吸波器(MPA),为实现强波吸收提供了一种新的策略。随后,Gong等^[28]提出了一种利用带有金属镜的金纳米三角形阵列来实现光吸收的方法,但吸收带宽受限。基于金属-绝缘体-金属(MIM)结构的超材料可以在具有单个或多个谐振器^[29-30]的结构中实现单波长或多波段的吸收。Cui等^[31]设计了锯齿金属绝缘体超材料吸波器,该器件可在宽红外光谱范围内实现高吸收。Bae等^[32]展示了一个由不同金属纳米尺度间隙组成的多尺度结构,该结构可在可见光和近红外范围内达到平均吸收率为91%的吸收。Wang等^[33]报道了一种基于微球单层模板的Ag/SiO₂叠加等离子体层结构的宽带光吸波器,在350~850 nm的波长范围内实现了90%以上的吸收。近年来的研究表明,通过将各种谐振器的频率混合在一起,可以扩大吸收带宽^[34]。此外,采用耐火金属替代贵金属作为吸波器的材料,不仅实现了宽带吸收,还确保了结构的高温耐性和稳定性^[35]。砷化镓(GaAs)因其耐高温、低温性能好、噪声小和抗辐射能力强等优点而广泛应用于宽带完美吸波器的设计^[36-37]。该技术在太阳能收集领域已得到验证。相变材料Ge₂Sb₂Te₅(GST)在可见光波段具有较大的介电

收稿日期: 2023-12-14; 修回日期: 2024-01-29; 录用日期: 2024-02-05; 网络首发日期: 2024-02-20

基金项目: 国家自然科学基金(62165004, 61805053)、广西自然科学基金(2023GXNSFAA026108)、桂林电子科技大学研究生创新项目(2022YCX047, 2021YCX040)、广西精密导航技术与应用重点实验室主任基金(DH202313)

通信作者: *hyang@guet.edu.cn

常数。GST可以在500 ps内从非晶态转换为晶态,晶态GST的介电常数更大。使用较低的电、热或光能即可实现GST从非晶态到晶态的转换。基于这些特点,GST适合构建高折射率的微腔谐振器,用于设计宽带高吸收率的吸波器^[38-39]。例如,Tian等^[38]提出了一种新型吸波器,通过将电介质-GST平面夹在GST立方体阵列和金属镜之间,实现了最高吸收率为99.94%的吸收峰。Wu等^[39]提出的吸波器以铁方环阵列的形式存在,通过电介质间隔层和相变材料(GST)层与铁反射器分离,在380~2000 nm的波长范围内实现了平均吸收率约为98%的吸收。

然而,之前的研究存在一些问题,如带宽较窄、结构复杂等。此外,对于同时使用GaAs和相变材料GST时的吸收性能缺乏研究。因此,本文基于三层MIM谐振器结构,利用GaAs和非晶态GST(A-GST),设计了一种多层空心圆盘堆叠结构的太阳能吸波器。分析了结构层数和每层介电材料(使用GaAs或A-GST)的不同对吸收率的影响,并以高吸收率和大工作带宽为目标优化结构参数;为了探究吸收的物理机制,分析了4个吸收峰处的相位参数、有效阻抗和电磁场分布;为了进一步探究吸波器的实用性,还分析了0°~50°的斜入射响应;最后,通过计算太阳能光谱加权吸收效率和有效热辐射率来评价该结构对太阳能的吸收和转换能力。

2 设计原理

超材料吸波器结构的复折射率 \tilde{n}_{eff} 可表示为

$$\tilde{n}_{\text{eff}} = n_{\text{eff}} + \kappa_{\text{eff}}, \quad (1)$$

式中: n_{eff} 为有效折射率; κ_{eff} 为消光系数。

MIM连续层隙等离子体谐振器从结构的末端(边缘)获得慢表面等离子体模式(间隙和短程表面等离子体模式)的多次反射,类似于传统的法布里-珀罗谐振器^[40-47],其具有与基本谐振模式^[41]相关的大电偶极矩,因此产生了显著的辐射损耗。MIM连续层隙等离子体谐振器的谐振条件也可以与任何其他法布里-珀罗型谐振器相同。

$$w \frac{2\pi}{\lambda} n_{\text{eff}} = m\pi - \varphi, \quad (2)$$

式中: λ 为自由空间波长; n_{eff} 为有效介电常数; m 是决定谐振模态阶数的整数; φ 是谐振器末端(条带的边缘)反射时的相位; w 为谐振腔的宽度。只考虑基本模态($m=1$),并定义相位参数 $\chi = \frac{1}{2} \left(1 - \frac{\varphi}{\pi} \right)$,则式(2)可化简为

$$wn_{\text{eff}} = \lambda\chi, \quad (3)$$

如果相移 $\varphi=0$,那么 $\chi=1/2$ (就像一个完美的导电镜)。

阻抗匹配理论(IMT)是探索超材料吸波器(MA)^[48]吸收原理的重要方法,当MA的有效阻抗 Z_{eff}

与自由空间的阻抗($Z_0=1$)相等时,MA产生完美吸收,其被称为超材料完美吸波器(MPA)。而该超材料的 Z_{eff} ^[49]可以表示为

$$Z_{\text{eff}} = \sqrt{\frac{(1+S_{11})^2 - S_{21}^2}{(1-S_{11})^2 - S_{21}^2}}, \quad (4)$$

式中: S_{11} 和 S_{21} 分别为与反射率和透射率相关的散射参数。

本文利用时域有限差分(FDTD)方法对所提出的吸波器进行了性能分析。对于宽带吸收,本文使用平均吸收率 \bar{A} 来评估吸收性能^[50]:

$$\bar{A} = \frac{\int_{\lambda_{\text{min}}}^{\lambda_{\text{max}}} A(\lambda) \cdot d\lambda}{\int_{\lambda_{\text{min}}}^{\lambda_{\text{max}}} d\lambda}, \quad (5)$$

式中: $A(\lambda)$ 为吸收率, $A(\lambda)=1-R(\lambda)-T(\lambda)$, $R(\lambda)$ 为反射率, $T(\lambda)$ 为透射率; λ_{max} 和 λ_{min} 分别表示吸收光谱的最大波长和最小波长。

由于实际太阳光谱的能量分布不均匀,因此需要通过计算太阳能光谱加权吸收效率 η_A 来评价所提出的吸波器对太阳能的吸收能力^[50]:

$$\eta_A = \frac{\int_{\lambda_{\text{min}}}^{\lambda_{\text{max}}} A(\lambda) I_{\text{AM1.5}}(\lambda) \cdot d\lambda}{\int_{\lambda_{\text{min}}}^{\lambda_{\text{max}}} I_{\text{AM1.5}}(\lambda) \cdot d\lambda}, \quad (6)$$

式中: $I_{\text{AM1.5}}(\lambda)$ 表示空气质量为1.5的全球光谱的入射太阳能。

有效热辐射率 η_E 是评价热辐射性能的一个重要参数^[50],可以根据普朗克定律进行计算:

$$\eta_E = \frac{\int_{\lambda_{\text{min}}}^{\lambda_{\text{max}}} \xi(\lambda) I_{\text{BE}}(\lambda, T) \cdot d\lambda}{\int_{\lambda_{\text{min}}}^{\lambda_{\text{max}}} I_{\text{BE}}(\lambda, T) \cdot d\lambda}, \quad (7)$$

式中: $I_{\text{BE}}(\lambda, T)$ 是理想黑体在波长 λ 和温度 T 下的热辐射功率; $\xi(\lambda)$ 是太阳能吸波器的辐射率,根据基尔霍夫定律^[51],它与 $A(\lambda)$ 相等。

3 结构与讨论

3.1 结构设计

图1为太阳能吸波器的示意图,结构以金属钨(W)为衬底,衬底上的多层堆叠圆盘分别由金属钛(Ti)、A-GST、GaAs组成,形成了三层MIM连续层隙等离子体强谐振器。其中A-GST或GaAs作为介电材料分隔W或Ti(顶层MIM谐振器使用A-GST作为介电材料,下面两层使用GaAs作为介电材料)。优化后的几何参数取值如表1所示,可以看到衬底W的厚度 h_0 较大可以有效地防止太阳光的透射 $[T(\lambda)=0]$,于是 $A(\lambda)=1-R(\lambda)$,本文后续的分析计算都以此为基础。

A-GST的介电常数 $\epsilon_{\text{A-GST}}$ 来自参考文献^[52]。Ti、

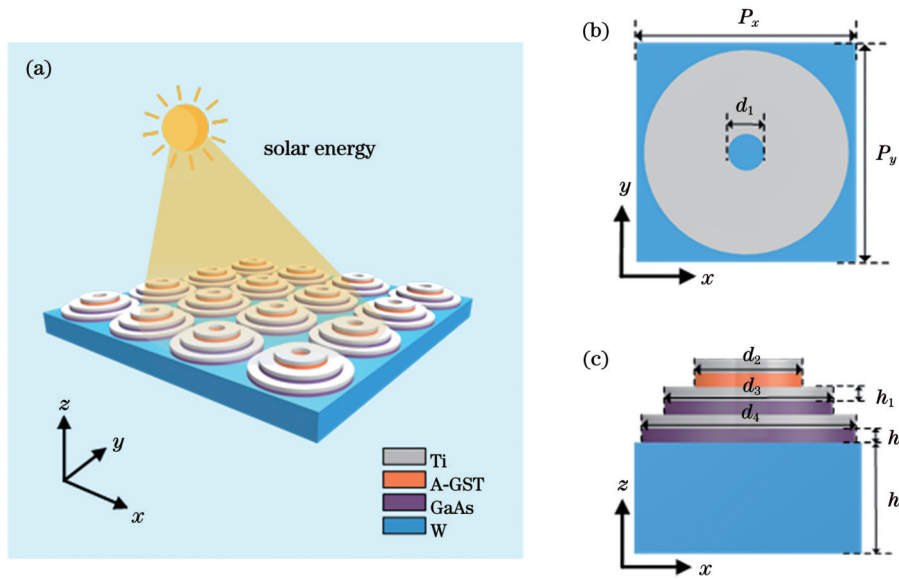


图 1 本文设计的太阳能吸波器。(a)整体结构图;(b)结构俯视图;(c)结构主视图

Fig. 1 Solar absorber designed in this paper. (a) Overall structural view; (b) top view of structure; (c) main view of structure

表 1 优化后的几何参数

Table 1 Optimized geometric parameters

Geometric parameter / μm	d_1	d_2	d_3	d_4	h_1 or h_2	h_3	P_x	P_y
Value	0.025	$0.5d_4$	$0.75d_4$	0.44	0.08	0.5	0.5	0.5

W 以及 GaAs 的介电常数是从小实验数据^[53]中得出的。太阳能吸波器的工作环境选择折射率为 1 的空气。将这些材料参数绘制为波长的函数,如图 2 所示。本文

使用 Matlab 软件对这些参数进行数值拟合,然后将拟合后的数据导入到 FDTD 软件中,建立相应的材料模型,最后进行模拟仿真。基于这些在以往的研究中被

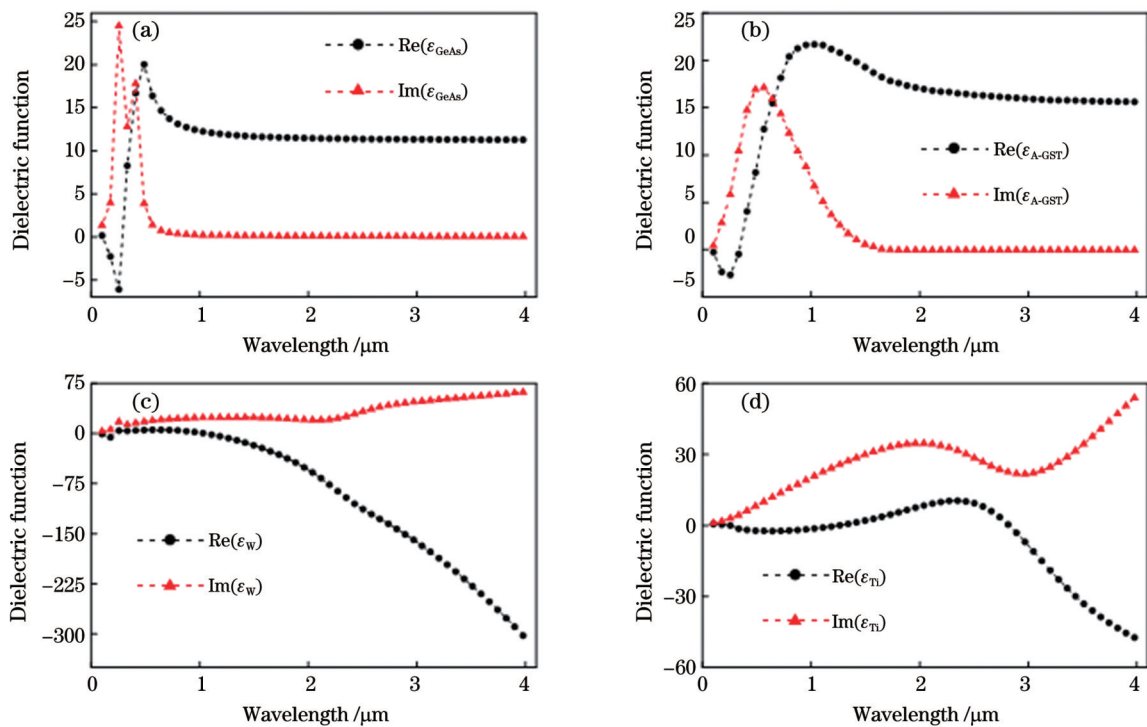


图 2 结构所用材料的介电常数与波长的关系图。(a) GeAs 介电函数;(b) A-GST 介电函数;(c) W 介电函数;(d) Ti 介电函数

Fig. 2 Relationship between dielectric constant of material used in structure and wavelength. (a) Dielectric function of GeAs; (b) dielectric function of A-GST; (c) dielectric function of W; (d) dielectric function of Ti

使用且验证过可靠性的材料数据来进行模拟仿真,确保了本研究的准确性和可指导性。另外,本文还探索了该制作工艺的流程。首先,通过抛光 W 表面来形成结构衬底。然后,使用等离子体增强型化学气相沉积(PECVD)方法沉积一定厚度的 GaAs 或 A-GST。接下来,通过热蒸镀的方式形成 Ti 薄膜。最后,通过重复沉积和热蒸镀的步骤,实现结构的二、三层^[54]。

3.2 讨论

图 3 反映了本研究所设计的吸波器吸收和转换太阳能的能力。其中图 3(a)表示的是吸收率 $A(\lambda)$ 、反射率 $R(\lambda)$ 和透射率 $T(\lambda)$ 的变化曲线,可以看出:结构存在较厚的 W 衬底,导致 $T(\lambda)$ 几乎为 0。因此,结构中的太阳能损失主要是由反射导致的。将图 3(a)中 4 个最高的吸收峰定义为 Mode 1~Mode 4;经过分析计算得出:在 $0.3\sim 2.5\ \mu\text{m}$ 的波长范围内,平均吸收率 \bar{A} 为 97.48%;在 $0.3\sim 4\ \mu\text{m}$ 的整个工作波段内,平均吸收率 \bar{A} 为 96.95%;吸收率大于 95% 的带宽为 $2.37\ \mu\text{m}$,吸

收率大于 90% 的带宽为 $3.57\ \mu\text{m}$,实现了超宽带、高效的太阳能吸收。图 3(b)表示的是在环境空气质量为 1.5(AM1.5)的全球光谱的入射下吸波器吸收太阳能的能力,其中蓝色部分为入射的太阳能(AM1.5),红色部分为结构吸收的太阳能,黑色部分为结构损失(反射)的太阳能,可以看出在整个工作波段内只有极少的太阳能损失,根据式(6)可以定量计算出太阳能光谱加权吸收效率 η_A 为 97.54%,这相比于之前的研究^[55-57]有了很大提高。图 3(c)比较了环境温度 $T=2000\ \text{K}$ 时吸波器与理想黑体的热辐射,可以看到两者的热辐射非常接近,这说明在 $T=2000\ \text{K}$ 时,结构几乎相当于一个理想黑体。根据式(7),计算了温度在 $300\sim 2000\ \text{K}$ 范围内的有效热辐射率 η_E 的变化情况,如图 3(d)所示,可以看到:随着温度的升高, η_E 的值也越来越大,并始终保持着 91.67% 以上的有效热辐射率,这进一步体现了吸波器优异的太阳能转换能力。

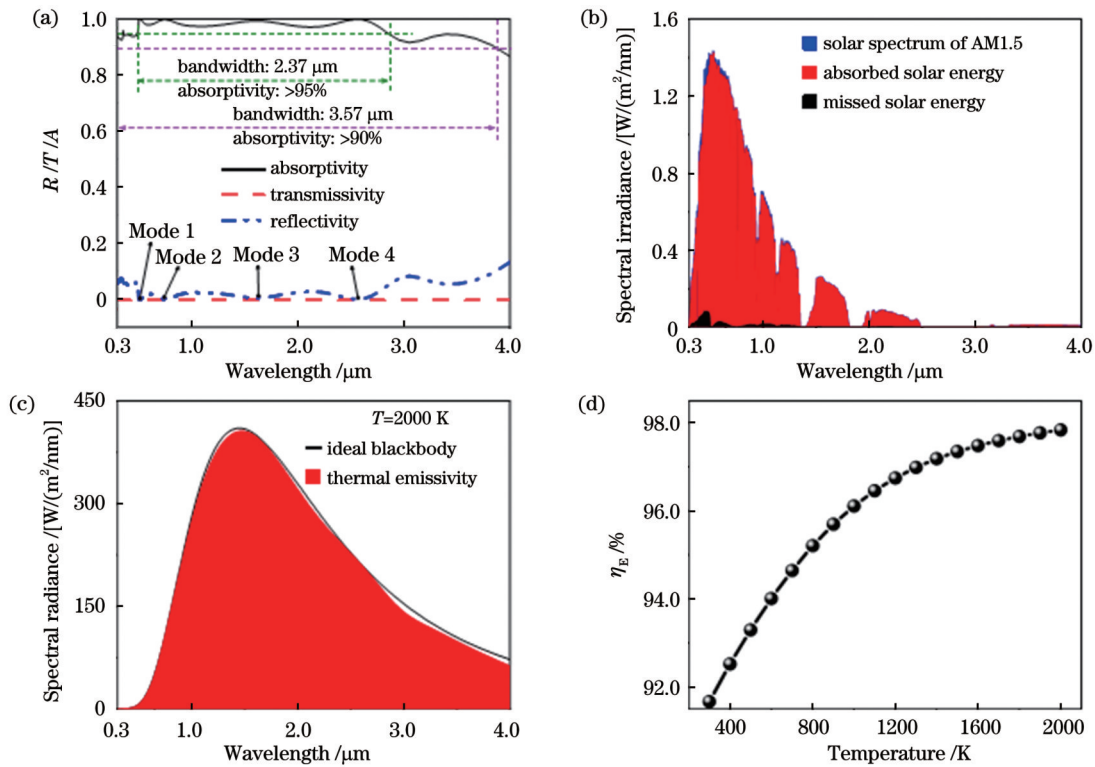


图 3 设计的太阳能吸波器的光谱和辐射特性。(a)在正常入射条件下的吸收率、反射率和透射率;(b)在 AM1.5 下的吸收光谱和损失光谱;(c)在 $T=2000\ \text{K}$ 下的热辐射效应;(d) $300\sim 2000\ \text{K}$ 时的有效热辐射率

Fig. 3 Spectral and radiation characteristics of designed solar absorber. (a) Absorptivity, reflectivity, and transmissivity of solar absorber under normal incidence conditions; (b) solar absorption and loss spectra under AM1.5; (c) thermal radiation effect at $T=2000\ \text{K}$; (d) effective thermal emissivity from $300\ \text{K}$ to $2000\ \text{K}$

图 4(a)绘制了根据式(1)~(3)计算出的相位参数 χ 和吸波器的消光系数 κ_{eff} 。由 χ 与谐振强度之间的关系^[58]可以得出:Mode 1 和 Mode 2 处的 χ 较大而 κ_{eff} 较小,所以这两处的高吸收率主要是由 MIM 结构谐振性导致的;随着波长的增加, χ 逐渐减小而 κ_{eff} 逐渐增大,也就意味着 Mode 3 和 Mode 4 两处的吸收峰主要依赖

于结构自身的材料损耗。从图 2(c)、(d)可以看出,正是由于材料 W 和 Ti 在 $2\sim 4\ \mu\text{m}$ 波长范围内的高损耗,结构的 κ_{eff} 得到显著提高,进而使得吸收带宽得到有效扩展。

图 4(b)为太阳能吸波器的有效阻抗 Z_{eff} 的实部和虚部,可以看到在 Mode 1~Mode 4 这 4 个吸收峰处的

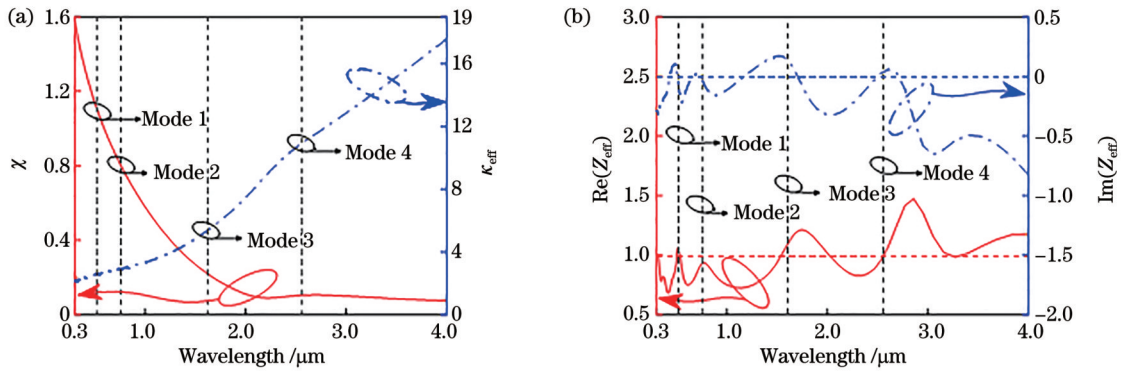


图 4 太阳能吸波器的三个主要参数与波长的关系。(a) 相位参数 χ 和消光系数 κ_{eff} ; (b) 有效阻抗 Z_{eff}

Fig. 4 Relationship between three main parameters of solar absorber and wavelength. (a) Phase parameter χ and extinction coefficient κ_{eff} ; (b) effective impedance Z_{eff}

$Z_{\text{eff}} \approx Z_0$, 而在吸收率较低的波长范围内, Z_{eff} 与 Z_0 的差值较大, 这与 IMT 的结论一致。

为了进一步探索吸收的物理机制, 还研究了 Mode 1~Mode 4 这 4 个吸收峰处 x - z 平面磁场、 y - z 平面电场的强度和矢量分布, 如图 5 所示。从图中可以看出: Mode 1 大部分的场都集中在上层 Ti 表面和中间的金属纳米盘间隙内, 所以此处的吸收峰是表面等离子体

共振 (SPR) 激发^[59] 和间隙模^[60] 的耦合结果; Mode 2 的场都在表层, 所以此处的吸收峰 SPR 起主要作用; Mode 3 的场分别集中在三层金属纳米盘间隙内, 所以此吸收峰处结构每层的间隙模式都被激发; Mode 4 的场主要集中在下层金属纳米盘间隙内, 所以此吸收峰处只有最下层的间隙模式被激发。总而言之, Mode 1~Mode 4 的联合作用, 有效增大了吸收带宽并提高了吸收率。

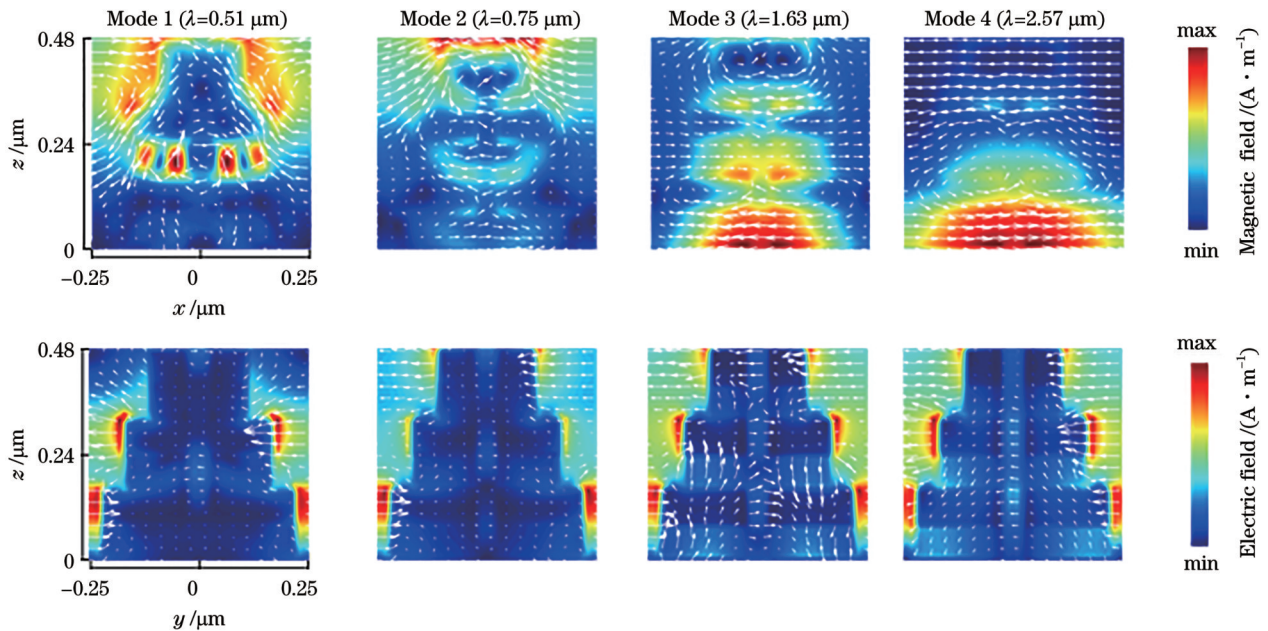


图 5 不同模式下的 x - z 平面磁场和 y - z 平面电场

Fig. 5 Distributions of x - z plane magnetic field and y - z plane electric field for different modes

本研究主要关注结构参数对吸收率的影响, 其中层数是一个重要的结构参数, 如图 6(a) 所示。除金属衬底 W 外, 结构每层都由 Ti 和 A-GST 或 GaAs 组成, 因此增加一层, 就多构成一层 MIM 谐振器, 从图 6(a) 的结果可以看出: 每增加一层 MIM 谐振器, 吸收率就会提高很多, 而当达到 3 层 MIM 强谐振器时, 吸收率便可以达到一个非常高的水平 ($\bar{A} = 96.95\%$)。值得注意的是, 当层数增加到 4 时, $0.3 \sim 4 \mu\text{m}$ 波长范围内

的 \bar{A} 为 97.04%。与 3 层结构相比, 4 层结构的吸收率并没有明显的提高。这是因为: 随着层数的增加, 顶层结构的尺寸变小, 导致谐振器从结构末端中获得间隙和短程表面等离子体模式的反射次数变少, 谐振强度被极大衰减^[61-65]。此外, 多增加的一层金属钛会使更多的太阳光被反射, 整体结构的吸收率并没有太大的提高。因此, 进一步增加层数并不会提高吸波器的性能, 反而增加了制造的难度和成本。

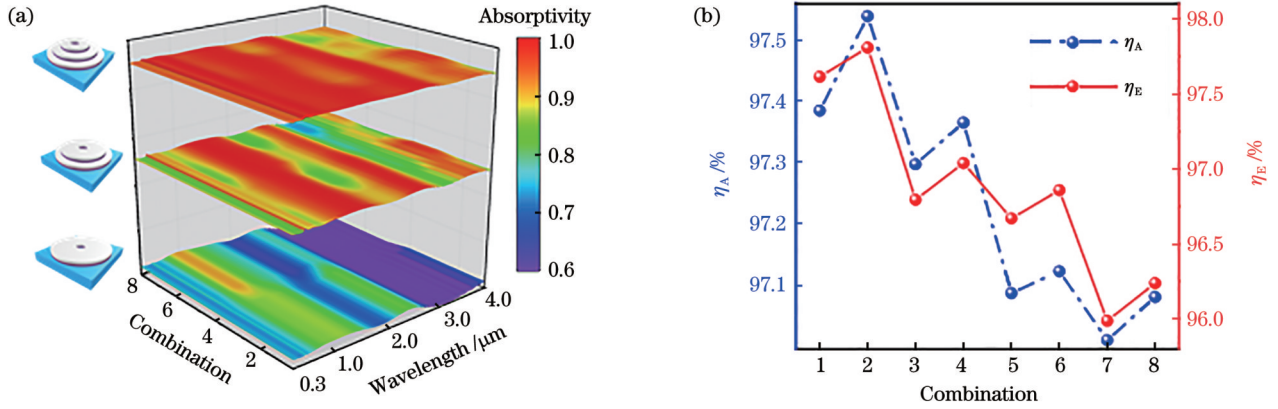


图6 结构层数和材料组合对吸波器性能的影响。(a)吸收率随结构层数和材料组合的变化;(b)三层结构时不同的材料组合对吸波器性能的影响

Fig. 6 Influence of number of structural layers and material combinations on performance of absorber. (a) Variation of absorption with number of structural layers and material combination; (b) influence of material combination on absorber performance in three-layer structures

需要注意的是,图6(a)还反映了每层的介电材料选择 A-GST 或 GaAs 时吸收率的变化情况,可以看出介电材料选择 A-GST 或 GaAs 对吸收率的影响并不是很大。为了更加清晰地分析 3 层 MIM 结构中每层介电材料的不同对吸收率的影响,计算了每层介电材料为 A-GST 或 GaAs 时 η_A 和 η_E 的变化情况,结果如图 6(b) 所示,横坐标为两种材料在 3 层结构中的排列组合,可以看出:不论是 A-GST 或 GaAs 单独作为介电材料还是两者同时被使用,太阳能吸波器都有很好的吸收性能,这表明 A-GST 和 GaAs 在太阳能吸波器的设计方面都有极高的应用价值,本研究选择顶层介电材料为 A-GST 而下面两层的介电材料为 GaAs

(Combination 为 2) 的结构来进行分析。

在实际应用场景中,光源的偏振角和入射角总是变化的,因此还需要分析吸波器对光源偏振角和入射角的响应。结构自身的对称性使其对光源的偏振角不敏感。图 7 为光源的入射角在 $0^\circ \sim 50^\circ$ 范围内变化时对吸收率的影响,可以看到:随着入射角的增加,结构的吸收率逐渐降低;在小角度入射下,由于 Mode 1~Mode 4 被有效激发,所以吸收率较高且变化不大;但在大角度入射下,Mode 1~Mode 4 被不同程度地限制,导致吸收率明显下降。整体而言,结构在 $0.3 \sim 2.5 \mu\text{m}$ 的波长范围内对入射角变化的响应相对稳定。

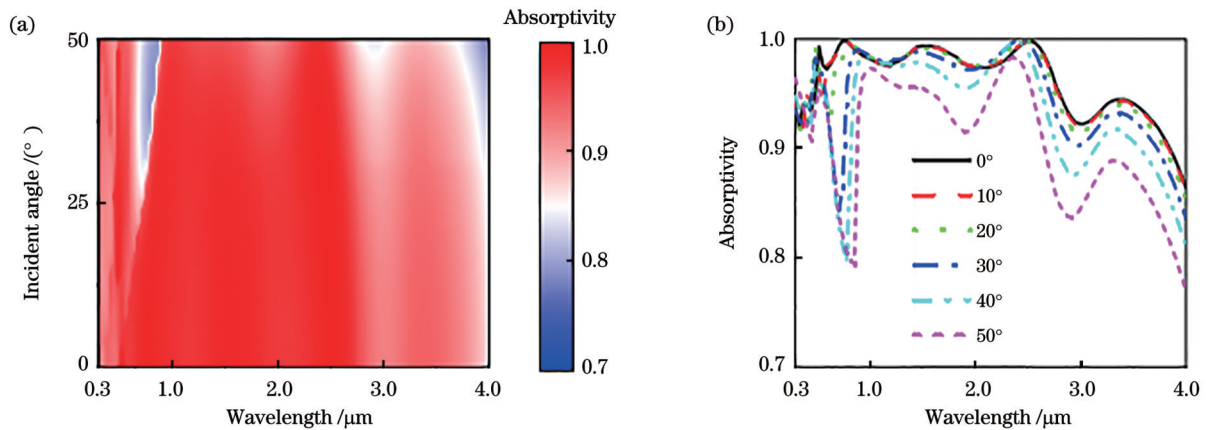


图 7 不同入射角对吸收率的影响

Fig. 7 Effect of angle of incidence on absorptivity

最后,将本研究与之前的工作进行比较,如表 2 所示。从比较结果可以看出,本研究在吸收带宽和吸收效率方面相比于之前报道的结果都有很大的优势,并且结合前文的分析可知,本研究在兼具了超宽带和高吸收率的同时,还极大降低了制造的复杂性和成本。

4 结 论

本文提出了一种基于 3 层 MIM 强谐振器结构的高吸收率超宽带太阳能吸波器。分析了每层 MIM 结构的介质材料,并讨论了 GaAs 或 A-GST 对吸收率的

表 2 本研究与近年来工作的比较
Table 2 Comparison of this study with work in recent years

Reference	Work wavelength / μm	Average absorptivity /%	Solar spectral weighted absorption efficiency /%
Ref. [55]	0.3–2.4	—	96.7
Ref. [56]	0.3–3	—	>90
Ref. [57]	0.288–2.16	96.56	95.89
Ref. [61]	0.4–2	97.9	—
Ref. [62]	0.4–2.5	90.4	—
This work	0.3–2.5	97.48	98.02
	0.3–4	96.95	97.54

影响。研究表明,这两种材料在太阳能吸波器设计方面都具有很高的应用价值。结构自身的对称性使其具备优良的偏振无关特性,有助于太阳光的吸收。此外,在 0.3~2.5 μm 的波长范围内,该结构对入射角变化也表现出稳定的响应。所设计的太阳能吸波器具有超宽带和高吸收率的特点,结构简单,大大降低了制造的复杂性和成本,因此在太阳能收集与转换、光伏器件和热发射器件等领域具有潜在的应用前景。

参 考 文 献

- [1] Bube F R. Fundamental of solar cells: photovoltaic solar energy conversion[M]. Amsterdam: Elsevier, 2012.
- [2] Granqvist C G, Niklasson G A. Solar energy materials for thermal applications: a primer[J]. Solar Energy Materials and Solar Cells, 2018, 180: 213-226.
- [3] Wang J J, Shi D L. Spectral selective and photothermal nano structured thin films for energy efficient windows[J]. Applied Energy, 2017, 208: 83-96.
- [4] Huen P, Daoud W A. Advances in hybrid solar photovoltaic and thermoelectric generators[J]. Renewable and Sustainable Energy Reviews, 2017, 72: 1295-1302.
- [5] Mauser K W, Kim S, Mitrovic S, et al. Resonant thermoelectric nanophotonics[J]. Nature Nanotechnology, 2017, 12(8): 770-775.
- [6] Sousa-Castillo A, Ameneiro-Prieto Ó, Comesana-Hermo M, et al. Hybrid plasmonic nanoresonators as efficient solar heat shields[J]. Nano Energy, 2017, 37: 118-125.
- [7] Wang X Z, He Y R, Liu X, et al. Solar steam generation through bio-inspired interface heating of broadband-absorbing plasmonic membranes[J]. Applied Energy, 2017, 195: 414-425.
- [8] Ghasemi H, Ni G, Marconnet A M, et al. Solar steam generation by heat localization[J]. Nature Communications, 2014, 5: 4449.
- [9] Zhou L, Tan Y L, Ji D X, et al. Self-assembly of highly efficient, broadband plasmonic absorbers for solar steam generation[J]. Science Advances, 2016, 2(4): e1501227.
- [10] Ni G, Li G, Boriskina S, et al. Steam generation under one sun enabled by a floating structure with thermal concentration[J]. Nature Energy, 2016, 1(9): 16126.
- [11] Politano A, Argurio P, di Profio G, et al. Photothermal membrane distillation for seawater desalination[J]. Advanced Materials, 2017, 29(2): 1603504.
- [12] Duan H L, Xuan Y M. Enhanced optical absorption of the plasmonic nanoshell suspension based on the solar photocatalytic hydrogen production system[J]. Applied Energy, 2014, 114: 22-29.
- [13] Jiang D Y, Yang W M, Tang A K. A refractory selective solar absorber for high performance thermochemical steam reforming[J]. Applied Energy, 2016, 170: 286-292.
- [14] Mola G T, Mthethwa M C, Hamed M S G, et al. Local surface plasmon resonance assisted energy harvesting in thin film organic solar cells[J]. Journal of Alloys and Compounds, 2021, 856: 158172.
- [15] Thaver Y, Oseni S O, Kaviyarasu K, et al. Metal nano-composite assisted photons harvesting in thin film organic photovoltaic[J]. Physica B: Condensed Matter, 2020, 582: 411844.
- [16] Adedeji M A, Hamed M S G, Mola G T. Light trapping using copper decorated nano-composite in the hole transport layer of organic solar cell[J]. Solar Energy, 2020, 203: 83-90.
- [17] Akbarzadeh S, Valipour M S. Heat transfer enhancement in parabolic trough collectors: a comprehensive review[J]. Renewable and Sustainable Energy Reviews, 2018, 92: 198-218.
- [18] El Nady J, Kashyout A B, Ebrahim S, et al. Nanoparticles Ni electroplating and black paint for solar collector applications[J]. Alexandria Engineering Journal, 2016, 55(2): 723-729.
- [19] Zhao Y, Alù A. Manipulating light polarization with ultrathin plasmonic metasurfaces[J]. Physical Review B, 2011, 84(20): 205428.
- [20] Luo X Q, Tan Z Y, Wang C, et al. A reflecting-type highly efficient terahertz cross-polarization converter based on metamaterials[J]. Chinese Optics Letters, 2019, 17(9): 093101.
- [21] Hadad Y, Sounas D L, Alu A. Space-time gradient metasurfaces[J]. Physical Review B, 2015, 92(10): 100304.
- [22] Zhou J H, Hu Y Z, Jiang T, et al. Ultrasensitive polarization-dependent terahertz modulation in hybrid perovskites plasmon-induced transparency devices[J]. Photonics Research, 2019, 7(9): 994-1002.
- [23] Sherrott M C, Hon P W C, Fountaine K T, et al. Experimental demonstration of $>230^\circ$ phase modulation in gate-tunable graphene-gold reconfigurable mid-infrared metasurfaces[J]. Nano Letters, 2017, 17(5): 3027-3034.
- [24] Yu P, Besteiro L V, Huang Y J, et al. Broadband metamaterial absorbers[J]. Advanced Optical Materials, 2019, 7(3): 1800995.
- [25] Fan R H, Xiong B, Peng R W, et al. Constructing metastructures with broadband electromagnetic functionality[J]. Advanced Materials, 2019, 32(27): 1904646.
- [26] Feng L, Huo P C, Liang Y Z, et al. Photonic metamaterial absorbers: morphology engineering and interdisciplinary applications[J]. Advanced Materials, 2020, 32(27): 1903787.
- [27] Landy N I, Sajuyigbe S, Mock J J, et al. Perfect metamaterial absorber[J]. Physical Review Letters, 2008, 100(20): 207402.
- [28] Gong J H, Yang F L, Zhang X P. A novel wideband optical absorber based on all-metal 2D gradient nanostructures[J].

- Journal of Physics D: Applied Physics, 2017, 50(45): 455105.
- [29] Aydin K, Ferry V E, Briggs R M, et al. Broadband polarization-independent resonant light absorption using ultrathin plasmonic super absorbers[J]. Nature Communications, 2011, 2: 517.
- [30] Lin K T, Chen H L, Lai Y S, et al. Loading effect-induced broadband perfect absorber based on single-layer structured metal film[J]. Nano Energy, 2017, 37: 61-73.
- [31] Cui Y X, Fung K H, Xu J, et al. Ultrabroadband light absorption by a sawtooth anisotropic metamaterial slab[J]. Nano Letters, 2012, 12(3): 1443-1447.
- [32] Bae K, Kang G M, Cho S K, et al. Flexible thin-film black gold membranes with ultrabroadband plasmonic nanofocusing for efficient solar vapour generation[J]. Nature Communications, 2015, 6: 10103.
- [33] Wang H F, Shi J X, Qian L Y, et al. Large-area broadband optical absorber fabricated by shadowing sphere lithography[J]. Optics Express, 2018, 26(6): 7507-7515.
- [34] Liu Z Q, Liu X S, Huang S, et al. Automatically acquired broadband plasmonic-metamaterial black absorber during the metallic film-formation[J]. ACS Applied Materials & Interfaces, 2015, 7(8): 4962-4968.
- [35] Ghobadi A, Hajian H, Rashed A R, et al. Tuning the metal filling fraction in metal-insulator-metal ultra-broadband perfect absorbers to maximize the absorption bandwidth[J]. Photonics Research, 2018, 6(3): 168-176.
- [36] Li Y Y, Liu Z Q, Pan P P, et al. Semiconductor-nanoantenna-assisted solar absorber for ultra-broadband light trapping[J]. Nanoscale Research Letters, 2020, 15(1): 76.
- [37] Li Y Y, Chen Q Q, Wu B, et al. Broadband perfect metamaterial absorber based on the gallium arsenide grating complex structure[J]. Results in Physics, 2019, 15: 102760.
- [38] Tian X M, Li Z Y. Visible-near infrared ultra-broadband polarization-independent metamaterial perfect absorber involving phase-change materials[J]. Photonics Research, 2016, 4(4): 146-152.
- [39] Wu J, Sun Y S, Wu B Y, et al. Broadband and wide-angle solar absorber for the visible and near-infrared frequencies[J]. Solar Energy, 2022, 238: 78-83.
- [40] Søndergaard T, Bozhevolnyi S. Slow-plasmon resonant nanostructures: scattering and field enhancements[J]. Physical Review B, 2007, 75(7): 073402.
- [41] Søndergaard T, Bozhevolnyi S. Slow-plasmon resonant nanostructures: scattering and field enhancements[J]. Physical Review B, 2007, 75(7): 073402.
- [42] Bozhevolnyi S I, Søndergaard T. General properties of slow-plasmon resonant nanostructures: nano-antennas and resonators [J]. Optics Express, 2007, 15(17): 10869-10877.
- [43] Søndergaard T, Bozhevolnyi S I. Metal nano-strip optical resonators[J]. Optics Express, 2007, 15(7): 4198-4204.
- [44] Søndergaard T, Bozhevolnyi S I. Strip and gap plasmon polariton optical resonators[J]. Physica Status Solidi (b), 2008, 245(1): 9-19.
- [45] Søndergaard T, Beermann J, Boltasseva A, et al. Slow-plasmon resonant-nanostrip antennas: analysis and demonstration [J]. Physical Review B, 2008, 77(11): 115420.
- [46] Jung J, Søndergaard T, Bozhevolnyi S I. Gap plasmon-polariton nanoresonators: scattering enhancement and launching of surface plasmon polaritons[J]. Physical Review B, 2009, 79(3): 035401.
- [47] Jung J, Søndergaard T, Beermann J, et al. Theoretical analysis and experimental demonstration of resonant light scattering from metal nanostrips on quartz[J]. Journal of the Optical Society of America B, 2008, 26(1): 121-124.
- [48] Liu S S, Ding F, Wu J, et al. A metamaterial absorber with centre-spin design and characteristic modes analysis[J]. Physica Scripta, 2022, 97(4): 045502.
- [49] Smith D R, Vier D C, Koschny T, et al. Electromagnetic parameter retrieval from inhomogeneous metamaterials[J]. Physical Review E, 2005, 71(3): 036617.
- [50] Guo L, Shi M F, Liu Y J, et al. High efficient ultra-broadband nanoscale solar energy absorber based on stacked bilayer nano-arrays structure[J]. Renewable Energy, 2023, 215: 119015.
- [51] Liu G Q, Liu X S, Chen J, et al. Near-unity, full-spectrum nanoscale solar absorbers and near-perfect blackbody emitters[J]. Solar Energy Materials and Solar Cells, 2019, 190: 20-29.
- [52] Chew L T, Zhou X L, Simpson R, et al. Chalcogenide active photonics[J]. Proceedings of SPIE, 2017, 10345: 103451B.
- [53] Palik E D. Handbook of optical constants of solids[M]. Amsterdam: Academic Press, 1985.
- [54] Xiao G L, Lai Z F, Yang H Y, et al. Tunable environment-enhanced mid-infrared absorber based on voltage modulation[J]. IEEE Photonics Journal, 2023, 15(5): 4601206.
- [55] Wang Z L, Liu Z, Zhang C, et al. Notched nanoring wideband absorber for total solar energy harvesting[J]. Solar Energy, 2022, 243: 153-162.
- [56] Qin F, Chen X F, Yi Z, et al. Ultra-broadband and wide-angle perfect solar absorber based on TiN nanodisk and Ti thin film structure[J]. Solar Energy Materials and Solar Cells, 2020, 211: 110535.
- [57] Zheng Y, Wu P H, Yang H, et al. High efficiency Titanium oxides and nitrides ultra-broadband solar energy absorber and thermal emitter from 200 nm to 2600 nm[J]. Optics & Laser Technology, 2022, 150: 108002.
- [58] Nielsen M G, Gramotnev D K, Pors A, et al. Continuous layer gap plasmon resonators[J]. Optics Express, 2011, 19(20): 19310-19322.
- [59] Wu B, Liu Z Q, Liu G Q, et al. An ultra-broadband, polarization and angle-insensitive metamaterial light absorber[J]. Journal of Physics D: Applied Physics, 2020, 53(9): 095106.
- [60] Wang Q, Li R, Gao X F, et al. Ultra-broadband absorber based on cascaded nanodisk arrays[J]. Chinese Physics B, 2022, 31(4): 040203.
- [61] Cai H Y, Wang M W, et al. Design of multilayer planar film structures for near-perfect absorption in the visible to near-infrared[J]. Optics Express, 2022, 30(20): 35219-35231.
- [62] Wang W H, Wang H B, Yu P, et al. Broadband thin-film and metamaterial absorbers using refractory vanadium nitride and their thermal stability[J]. Optics Express, 2021, 29(21): 33456-33466.
- [63] 王杨, 轩雪飞, 朱路, 等. 超宽带高吸收超材料太阳能吸收器设计[J]. 中国激光, 2022, 49(9): 0903001.
Wang Y, Xuan X F, Zhu L, et al. Design of ultra-broadband and high-absorption metamaterial solar absorber[J]. Chinese Journal of Lasers, 2022, 49(9): 0903001.
- [64] 何胜军, 江孝伟. 双通道偏振无关介电窄带超材料吸收器 [J]. 激光与光电子学进展, 2022, 59(3): 0316005.
He S J, Jiang X W. Dual channel polarization independent dielectric narrow bandwidth metamaterial absorber[J]. Laser & Optoelectronics Progress, 2022, 59(3): 0316005.
- [65] 谢朝辉, 屈薇薇, 邓璇, 等. 太赫兹超材料吸收器的逆向设计 [J]. 光学学报, 2023, 43(13): 1316001.
Xie Z H, Qu W W, Deng H, et al. Reverse design of terahertz metamaterial absorber[J]. Acta Optica Sinica, 2023, 43(13): 1316001.

High Absorptivity Solar Absorber Based on MIM Resonant Structure

Xiao Gongli¹, Chen Kang¹, Yang Hongyan^{2*}, Zhang Jiarong¹, Li Miao¹, Liu Xingpeng¹,
Chen Zanhui¹

¹Key Laboratory of Microelectronic Devices and Integrated Circuits of Guangxi Colleges, School of Information and Communication, Guilin University of Electronic Technology, Guilin 541004, Guangxi, China;

²School of Optoelectronic Engineering, Guilin University of Electronic Technology, Guilin 541004, Guangxi, China

Abstract

Objective The development and utilization of new energy sources has always been an important human research field. As a green and renewable energy source, solar energy provides an effective way to alleviate the energy crisis. To date, many methods have been proposed for converting solar radiation into other forms of energy and applications, such as photovoltaics and solar cells, light and heat generators, thermoelectric power generation and solar steam power generation, seawater desalination, and photochemical and photocatalytic reactions. Notably, efficient solar energy capture is the key to realizing these applications. Therefore, the ultimate goal of investigating solar absorbers is to completely absorb solar radiation over the entire spectral range and to employ as little photosensitive material as possible. In the past few years, several methods for efficient absorption of solar radiation have been investigated. For example, black paint is widely adopted but exhibits high absorptivity only in ultraviolet and visible wavelengths, which wastes about 28% of solar energy. However, with technological advancement, metamaterials open up many new ways to manipulate electromagnetic waves, and they have many unique optical properties and have been shown to control the polarization state, amplitude, and phase of electromagnetic waves. Changing the light amplitude is a way to control light absorption. Therefore, it is important to study the perfect absorbers for solar energy based on metamaterials.

Methods We design a solar absorber with a multi-layer hollow disk stacked structure based on a metal-dielectric-metal (MIM) resonator structure utilizing GaAs and amorphous GST (A-GST). Additionally, the designed solar absorber is simulated and theoretically analyzed using the finite difference method in time domain (FDTD) and data analysis software Matlab. First, the effect of the structural layer number and the difference in dielectric material per layer (using GaAs or A-GST) on the absorption is analyzed, and the structural parameters are optimized for achieving high absorptivity and broad operating bandwidth. Second, the phase parameters, effective impedance, and electromagnetic field strength and vector distributions at the four absorption peaks are analyzed to investigate the physical absorption mechanism. Then, the oblique incidence response from 0° to 50° is also analyzed to further explore the practicality of the absorber. Finally, the structure's ability to absorb and convert solar energy is evaluated by calculating the solar spectrum-weighted absorption efficiency and effective thermal emissivity.

Results and Discussions The results of the study show that both GaAs and amorphous state GST materials are extremely helpful in the design of solar absorbers (Fig. 6). The structure shows an average absorptivity of 97.48% in the wavelength range of 0.3–2.5 μm and a solar spectrum-weighted absorption efficiency of 98.02%. Meanwhile, the average absorptivity is 96.95% over the entire operating band from 0.3 μm to 4 μm , and the solar spectrum-weighted absorption efficiency is 97.54% (Fig. 6). The bandwidth is 2.37 μm for absorptivity greater than 95% and 3.57 μm for absorptivity greater than 90% (Fig. 3). The symmetry of the structure itself gives it excellent polarization-independent properties (Fig. 1), which is very favorable for solar absorption. Additionally, in the wavelength range of 0.3–2.5 μm , the structure also exhibits a stable response to changes in the incidence angle (Fig. 7). The designed solar absorber characterized by ultra-broadband and high absorptivity can provide tremendous advantages in absorption bandwidth and absorption efficiency over previously reported results (Table 2), and also greatly reduce the complexity and cost of fabrication due to the simplicity of the structure.

Conclusions We propose a high-absorptivity ultra-broadband solar absorber based on a three-layer MIM strong resonator structure. The dielectric material for each layer of the MIM structure is analyzed with the effect of GaAs or A-GST on the absorptivity discussed. The results of the study show that both materials are highly applicable in the design of solar absorbers. The symmetry of the structure itself gives it excellent polarization-independent properties, which are very favorable for solar absorption. The designed solar absorber is characterized by ultra-broadband and high absorptivity with a simple structure, which greatly reduces the complexity and cost of fabrication. Therefore, it has potential applications in solar energy collection and conversion, photovoltaic devices, and thermal emitter devices.

Key words surface optics; solar absorber; MIM resonant structure; high absorptivity; ultra-broadband; polarization independence